RAPID COMMUNICATIONS

PHYSICAL REVIEW B VOLUME 32, NUMBER 12 15 DECEMBER 1985

New evidence of extensive valence-band mixing in GaAs quantum wells through excitation photoluminescence studies

R. C. Miller and A. C. Gossard
AT&T Bell Laboratories, Murray Hill, New Jersey 07974

G. D. Sanders and Yia-Chung Chang
Department of Physics and Materials Research Laboratory, University of Illinois at Urbana-Champaign, 1110 West Green Street, Urbana, Illinois 61801

J. N. Schulman
Hughes Research Laboratories, 3011 Malibu Canyon Road, Malibu, California 90265
(Received 15 October 1985)

A well-resolved split peak at the $n=2$ heavy-hole exciton transition observed at low temperatures in excitation spectra is characteristic of ≈ 100-Å-wide square GaAs quantum wells of high quality. Theoretical calculations using a multiband effective-mass approach demonstrate that the lower-energy component arises from transitions involving the $n=1$ light hole and $n=2$ electron. This strong transition, which is normally parity forbidden for symmetric square wells, becomes allowed due to valence-band mixing and along with the other transitions observed is quantitatively accounted for by the theory.

There have been several publications recently emphasizing extensive mixing of the few lowest valence-band steps in the two-dimensional density of states of GaAs quantum wells with $Al_xGa_{1-x}As$ barriers.[1-6] However, there has been little experimental evidence for this from conventional photoluminescence studies except for the prominent parity-allowed exciton transition between the $n=1$ electron level and the $n=3$ heavy-hole level denoted E_{13h}.[7,8] This $\Delta n \neq 0$ transition, first observed but not identified by Dingle,[9] exhibits a strength with square GaAs wells which is orders of magnitude larger than that calculated using a simple single-band particle-in-a-box model.[10] On the other hand, the energies at which the E_{13h} exciton transition occurs are given correctly if one utilizes the recently proposed valence-band offsets ($\Delta E_v \approx 0.4\Delta E_g$)[8] and a [100] heavy-hole effective mass of $0.34m_0$ for this system.[8,11] However, a realistic tight-binding calculation[3] and a multiband effective-mass approach,[6] both of which include mixing of light- and heavy-hole states, lead to an E_{13h} transition at essentially the correct energy and of reasonable strength if one utilizes the band offsets and heavy-hole effective-mass given above.

These theories also predict for square GaAs quantum wells other exciton transitions with $\Delta n \neq 0$ of significant strength. This Rapid Communication emphasizes the experimental observation with square GaAs quantum wells of one of these normally "parity-forbidden" transitions with a strength comparable to a $\Delta n = 0$ transition and a quantitative theoretical explanation in terms of the multiband effective mass approach.[6] It has been known for about six years that high-quality GaAs quantum wells of width $L \approx 100$ Å and $x = 0.3$ $Al_xGa_{1-x}As$ barriers exhibited a peak in the region of the $n=2$ electron-heavy-hole transition, E_{2h}, which had two well-resolved components of comparable strength separated by ≈ 10 meV.[12] This structure has been observed with samples from a number of different wafers and has defied explanation in terms of the simple particle-in-a-box model. Examples of this are shown in Figs. 1 and 2 for samples grown in the [100] direction by molecular-beam epitaxy. Also included in these figures are the theoretically predicted absorption spectra based on a multiband effective-mass model as described in Ref. 6.

The multiband effective-mass theory of quantum well absorption treats electron and hole states separately. The spin-$\frac{1}{2}$ electron states are obtained using the simple particle-in-a-box model. The effective-mass Hamiltonian for the spin-$\frac{3}{2}$ hole operates on a four-component spin or wave function with column index $m = \frac{3}{2}, \frac{1}{2}, -\frac{1}{2}$, and $-\frac{3}{2}$. In the effective-mass approximation $(H_h)_{mm'} = T_{m,m'} + V_h(Z)\delta_{mm'}$, where $V_h(Z)$ is a finite square-well potential for the holes and $T_{m,m'}$ is the kinetic energy matrix given in the limit of infinite spin-orbit splitting by the $\mathbf{k}\cdot\mathbf{p}$ expression of Luttinger and Kohn.[13] Thus the treatment of the valence-band structure is similar to that reported by Fasolino and Altarelli.[14] The resulting Schrödinger equations for free electrons and holes are solved using a variational method. Coupling between heavy- ($j=\frac{3}{2}$) and light- ($j=\frac{1}{2}$) hole subbands due to the off-diagonal components of the hole kinetic energy operator $T_{m,m'}$ is included. Due to the strong coupling between heavy- and light-hole bands the optical matrix elements are rapidly varying functions of the wave vector $\mathbf{k}$ and all transitions between different subbands are dipole allowed.[2,3,6] Thus excitons derived from various subbands give rise to peak structures below the absorption edges of each of the subband-to-subband transitions. A very strong "forbidden" transition becomes possible when the energy of the valence subband involved is close to that of another valence subband which participates in an allowed transition as in the case discussed here.

The exciton binding energies and envelope functions are obtained by solving a two-dimensional effective-mass equation which incorporates effects of nonparabolic subband structure and valence-band mixing.[6,15] The input Luttinger parameters used for this calculation were obtained from the magnetoreflection measurements of Bimberg which give a heavy-hole effective mass $m_h^*/m_0 = 0.38$ and a light-hole effective mass $m_l^*/m_0 = 0.090$.[11] Making use of the computed

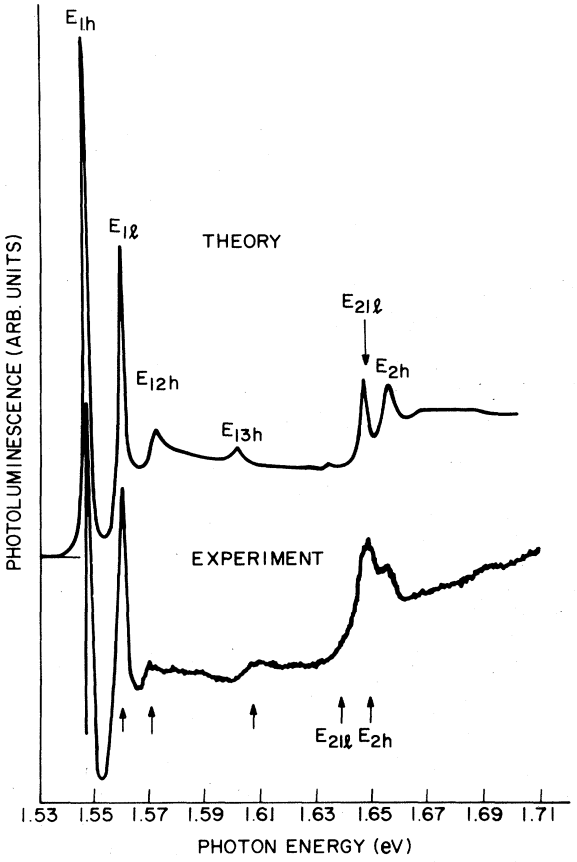

FIG. 1. Experimental excitation spectrum and theoretical absorption spectrum for a GaAs multiquantum well sample at 5 K with 102-Å-wide wells. The major calculated absorption peaks are labeled as described in the text. Arrows below the experimental curve indicate the energies of the exciton transitions estimated from the single-band simple particle-in-a-box model which does not explain the strength of the $\Delta n \neq 0$ transitions. The multiband effective-mass approach that includes valence-band mixing results in a theoretical curve that explains the energies and strengths of the various observed transitions.

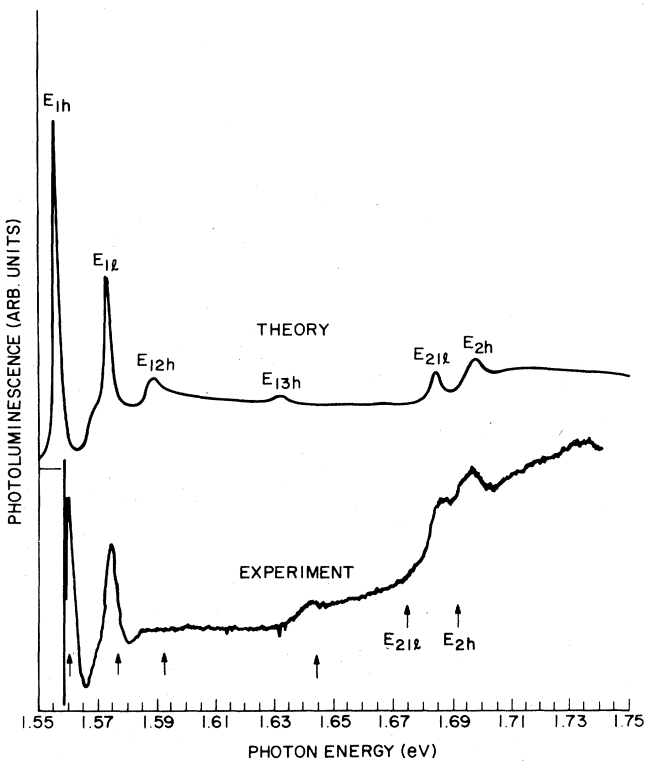

FIG. 2. Spectra similar to those described in the figure caption for Fig. 1 but for a sample with 81-Å-wide GaAs quantum wells. As with Fig. 1, the theoretical curve explains the two peaks near 1.69 eV including the change in their relative strengths with the change in L from 102 to 81 Å. A comparison of the transitions indicated by the arrows below the experimental curve with the data again illustrates the deficiency of the simple particle-in-a-box model. It appears that the E_{12h} transition may not be observed with the structure on the high-energy side of the experimental E_{1l} peak being due to the onset of the E_{1l} exciton continuum.

effective-mass envelope functions and energies one can obtain optical matrix elements and the theoretical absorption spectra of Figs. 1 and 2 using Fermi's golden rule.

To approximate the experimental situation, the band-to-band and exciton absorption spectra are broadened by Lorentzian functions of half-widths Γ_b and Γ_x. The widths of the exciton lines Γ_x, which depend on their lifetimes, and the band-to-band linewidths Γ_b are chosen to match the experimental data. We have found that reasonable choices of Γ_x and Γ_b are given by the relations $\Gamma_{x,b} = c_0 n_e n_h$ meV, where n_e and n_h are principle quantum numbers for electrons and holes and c_0 is a dimensionless constant of order unity. In generating the theoretical curves in Figs. 1 and 2 we adjusted c_0 until the linewidths of E_{1l} matched the data, i.e., $c_0 = 0.75$ and 1.0, respectively.

The structure used for Fig. 1 consisted of 78 GaAs wells of width $L = 102$ Å, and 207-Å-thick $x = 0.27$ alloy barriers as estimated from the deposition rates measured during the growth of the wafer. These estimates are believed accurate within $\pm 6\%$. Figure 1 shows the excitation spectrum at 5 K with 18 mW/cm^2 of incident intensity from a cw tunable dye laser scanned in energy with the photoluminescence (PL) detected at 1.547 eV. The PL spectrum (not shown) was 5.5 meV wide, full width at half maximum (FWHM), and consisted of two sharp peaks separated by 1.2 meV. The lower-energy peak has been attributed to biexcitons.[16] Of most interest in Fig. 1 is the double peak at ≈ 1.65 eV. The $\Delta n = 0$ transitions are indicated by E_{ij}, where $i = n$, and j either h or l gives the type of hole, heavy or light, respectively. The $\Delta n \neq 0$ transitions are identified by E_{ijk}, where $i = n$ for the electron, $j = n$ for the hole, and k its character either h or l. The arrows beneath the experimental curve show the "best fit" to the data using the recently revised quantum well parameters given in Ref. 8 and L as an adjustable parameter. The calculation assumes the same binding energy for all excitons derived from a given series of light- or heavy-hole subbands.[17,18] The value of L used was 99 Å, i.e., one monolayer more narrow (3%) than, but well within the range of that estimated from the growth parameters. While this fit is excellent except for E_{21l}, it cannot explain the strength of the $\Delta n \neq 0$ transitions and hence the structure near E_{2h}. The structure observed at E_{12h} may contain contributions from the onset of the E_{1l} exciton continuum.[17] However, as shown by the upper curve in Fig. 1,

the multiband effective-mass calculation using the same quantum well parameters gives excellent predictions of both the energies of the various transitions and reasonable strengths for them. The binding energies of the E_{2h} and E_{2l} excitons predicted from this calculation are found to be smaller than that of the E_{1h} exciton. Including the variation in exciton binding energy for different peaks yields a result in better agreement with the data. Note that in this case, the E_{2l} "parity-forbidden" exciton transition has a strength comparable to that of the E_{2h} allowed transition. The peak labeled E_{13h} predicted by the theory with $m_h^* = 0.38 m_0$ appears slightly lower in energy, ≈ 3 meV, than the corresponding experimental peak. On the other hand, if one uses $m_h^* = 0.34 m_0$,[8] the energies of the experimental and calculated E_{13h} peaks are the same.

Figure 2 shows the excitation spectrum at 5 K for a sample with 81 wells of width 81 Å separated by 205-Å-wide $x = 0.26$ alloy barriers. As above, the quantum well parameters are believed accurate to within $\pm 6\%$. For these data, detection was set at 1.559 eV and the incident beam at 27 mW/cm^2 scanned in energy. The PL peak was 6 meV wide, FWHM, and as above, it showed evidence of biexcitons.[16] The "best fit" to the data obtained with the usual simple model as discussed above and $L = 80$ Å is shown by the arrows beneath the experimental data. As noted earlier, this model cannot explain the strengths of the $\Delta n \neq 0$ transitions. It appears that E_{12h} may not be observed with this sample and that the shoulder on the high-energy side of E_{1l} is due to the E_{1l} exciton continuum. Also, it is more evident here than in Fig. 1 that the simple model, as expected, does not yield the correct energies of the exciton transitions which involve the subbands that are severely perturbed due to their proximity, e.g., E_{2l} and E_{2h}. Again the theoretical (upper) curve predicts all the features observed except for E_{12h}. A possible explanation for this discrepancy is that the E_{12h} exciton state may interact strongly with the continuum states corresponding to excitations of electrons in the first subband and holes in the second subband, because both the energies and the wave vectors of these states are very close to each other. Such interaction may further broaden the E_{12h} peak and make it less pronounced in the experimental spectra. The theory yields the observed L dependence of the oscillator strengths of the E_{2l} and E_{2h} transitions and shows, for example, that the maximum E_{2l} oscillator strength occurs for $L \approx 100$ Å as in Fig. 1.[15]

Careful photoluminescence studies with circular polarization excitation and detection techniques have verified previously that the hole assignments for the $\Delta n = 0$ and E_{13h} transitions are indeed as labeled in Figs. 1 and 2.[7,19] Similar studies carried out for the spectral region of the E_{2l} and E_{2h} peaks show very little if any difference in the heavy-hole character of the polarization of these two peaks. This demonstrates that the E_{2l} peak derives its strength and polarization from the $n = 2$ heavy-hole level as required by the theory.

In conclusion, we have found convincing new evidence that extensive valence-band mixing can occur in GaAs semiconductor quantum wells. This band-mixing effect can give rise to a very strong "forbidden" transition as the energy of the valence subband involved becomes close to that of another valence subband which participates in an allowed transition. The condition is most favorably met by the first light-hole and the second heavy-hole subband. We have shown that the multiband effective-mass approach including the valence-band mixing is able to account for the various exciton transitions observed in the excitation spectra of ≈ 100 Å GaAs quantum well samples, especially the very strong normally "parity-forbidden" exciton transition near the $n = 2$ heavy-hole $\Delta n = 0$ transition.

The research at the University of Illinois was supported by the Office of Naval Research under Contract No. N00014-81-K-0430.

[1] Y. C. Chang and J. N. Schulman, Appl. Phys. Lett. **43**, 536 (1983).
[2] J. N. Schulman and Y. C. Chang, Phys. Rev. B **31**, 2056 (1985).
[3] Y. C. Chang and J. N. Schulman, Phys. Rev. B **31**, 2069 (1985).
[4] M. Altarelli, J. Lumin. **30**, 472 (1985).
[5] R. Sooryakumar, D. S. Chemla, A. Pinczuk, A. C. Gossard, W. Wiegmann, and L. J. Sham, Solid State Commun. **54**, 859 (1985).
[6] G. D. Sanders and Y. C. Chang, Phys. Rev. B **31**, 6892 (1985).
[7] R. C. Miller, D. A. Kleinman, W. A. Nordland, Jr., and A. C. Gossard, Phys. Rev. B **22**, 863 (1980).
[8] R. C. Miller, D. A. Kleinman, and A. C. Gossard, Phys. Rev. B **29**, 7085 (1984). This is the first of many references from 1984 on which support the result $\Delta E_v \approx 0.4 \Delta E_g$.
[9] R. Dingle, in *Festkörperprobleme,* edited by J. Treusch, Advances in Solid State Physics, Vol. 15 (Pergamon, New York, 1975), p. 21.
[10] R. C. Miller, A. C. Gossard, D. A. Kleinman, and O. Munteanu, Phys. Rev. B **29**, 3740 (1984).
[11] M. S. Skolnick, A. K. Jain, R. A. Stradling, J. Leotin, J. C. Ousset, and S. Askenazy, J. Phys. C **9**, 2809 (1976), $m_h^*/m_0[100] = 0.40 \pm 0.08$; D. Bimberg, in *Festkörperprobleme,* edited by J. Treusch, Advances in Solid State Physics, Vol. 17 (Pergamon, New York, 1977), p. 195, $m_h^*/m_0[100] = 0.38 \pm 0.05$.
[12] R. C. Miller (unpublished).
[13] J. J. Luttinger and W. Kohn, Phys. Rev. **97**, 869 (1955).
[14] A. Fasolino and M. Altarelli, *Two-Dimensional Systems, Heterostructures, and Superlattices* (Springer, Berlin, 1984), p. 176.
[15] G. D. Sanders and Y. C. Chang, Phys. Rev. B **32**, 5517 (1985).
[16] R. C. Miller, D. A. Kleinman, A. C. Gossard, and O. Munteanu, Phys. Rev. B **25**, 6545 (1982).
[17] R. C. Miller, D. A. Kleinman, W. T. Tsang, and A. C. Gossard, Phys. Rev. B **24**, 1134 (1981).
[18] R. L. Greene, K. K. Bajaj, and D. E. Phelps, Phys. Rev. B **29**, 1807 (1984).
[19] C. Weisbuch, R. C. Miller, R. Dingle, A. C. Gossard, and W. Wiegmann, Solid State Commun. **37**, 219 (1981).